Magnetic coupling with 3D knitted helical coils

K. Fobelets[1], K.S. Sareen[1] and K. Thielemans[2]

[1]Optical and Semiconductor Devices Group, Electrical and Electronic Engineering Department, Imperial College London, Exhibition Road, SW7 2AZ London, UK (e-mail: k.fobelets@imperial.ac.uk).
[2]Institute of Nuclear Medicine, UCL, UCL Hospital, NW1 2BU London, UK
[3]Centre for Medical Imaging Computing, UCL, 90 High Holborn, London, WC1V 6LJ , UK

Abstract—Continuous power supply for wearable electronics can be facilitated using wireless power transfer (WPT). We use a 3D knitted helical coil as the receiver coil in the wrist or the waist of a garment. This 3D knitted helical coil is a novel approach to integrate coils in garments that maintains full flexibility of the garment. Measurements and simulations of coil-coil coupling give compelling evidence of the feasibility of this approach for wearable WTP. The coupling factor between a closely wound and knitted coil is found to be ~0.25 and ~0.55 for adjacent coils for a knit in the border of a cuff and waist, respectively. Using a simple circuit, we demonstrate a 30% efficiency between a closely wound transmitter coil worn on the wrist and a 3D knitted helical receiver coil integrated in the cuff of a garment at 6 mm distance.

Index Terms—knitted coils, e-textiles, flexible coils, magnetic coupling, WPT

1. Introduction

Smart wearable garments are increasing in popularity, driven by body-sensor-networks [1] often aimed at real-time and continuous fitness and health monitoring applications [2]. Commercial products have been launched, exploiting these new opportunities and the market forecast in smart wearables looks very promising [3]. Notwithstanding this success, there are still many problems remaining before large scale uptake in the consumer market or medical diagnostics will be achieved. The integration of electronics into fabrics and yarns often reduces their wearability and aesthetics and the need for power supplies reduces their autonomy. These two challenges are directly related to the contents of this manuscript. There is a need for portable power supplies to avoid interruption of the sensing activities to charge a battery pack at the mains. One method to achieve this is wireless power transfer (WPT) [4,5] between a primary body-worn coil connected to a small battery and a secondary flexible wearable coil in a garment that picks up the power and transfers it to the body sensors' location. Different approaches have been proposed for integrating coils into garments. Spiral inductors have been screen printed on fabrics making flat coils [6,7,8]. In [6] planar coils were integrated into fabrics by printing conductive tracks on top of a fabric in a 14 cm × 14 cm area. The printed coil retained most of the elasticity and flexibility of a traditional garment and successful DC/DC WPT was demonstrated with an efficiency of 37% at a distance of 5 mm. Equivalently, spiral inductors can be made by embroidering with conductive wire [6,9,10]. In [11] and [12] resonant coils were made of conductive yarn embroidered on nonwoven polyester fabric with a maximum transmission efficiency of ~50% when worn around the ankle or wrist. The embroidered receiver coil [11] was 14 cm in diameter and had 10 turns. The transfer power efficiency was on average 45% with a distance between coils of less than 6.5 cm. In addition, the power in these applications was scavenged from body movement making it completely autonomous. Similarly, thermoelectrics, exploiting body heat [13], can be used as a power scavenging method.

Whilst woven and non-woven fabrics are used in planar coils, in [14] metal was inlaid into the bottom of a knitted "jumper", making a helical coil with 28 turns and a diameter of 58 cm. This approach loses the flexibility that is traditionally expected from a garment but showed an efficiency of 30% at a distance of 20 cm. The cylindrical nature of many body parts offers opportunities for WTP using 3D helical coils integrated in clothing knitted in cylinders fitting the body. In this work, we investigate the magnetic coupling between a wound helical coil or a 3D knitted helical coil and another 3D knitted helical coil. Magnetic coupling is the basic requirement for WPT. In our implementation, we knit cotton yarn and a thin insulated Cu wire simultaneously in the round as proposed originally in [15] and illustrated in Fig. 1. Circular weft knitting must be used such that the metal wire runs continuously through all knitted rows to make the windings of the helical coil. We have shown that these round-knitted 3D helical coils behave similarly to classical wound helical coils for windings up to at least $N = 10$ (N is equivalent to the number of knitted rows). The resistance of the knitted coil is higher than a classical wound helical coil due to the horseshoe character of the stitches in the knit. On the other hand, this horseshoe character gives the knit its elasticity notwithstanding the non-elasticity of the yarn and wire. We use thin Cu wire with polymer insulation (total diameter ~250 μm) that is inexpensive and easily bendable. We analyze the performance of individual knitted coils and the coupling between two coils in function of knit parameters: stitch type, gauge, number of windings N, coil diameter D and distance between coils d. We extract empirical coil and coupling equations from the measurements. In addition, we extend our knitted coil model [15], implemented in Mathematica[TM] [16], to simulate the magnetic coupling between two coils as a function of distance and diameter by implementing the Neumann equation for mutual magnetic coupling. The horseshoe undulations of the stitches are parameterized on top of a helix. The metal wire in the simulations does not have a thickness but the forwards and backwards movement of each stitch, because of the cotton yarn thickness, is taken into account. Geometrical parameters used in the simulations are based on measurement of the knitted coil. This implementation gives information on coupling behavior that is specific to knitted coils and can be used to support knit design for future applications. The simulation results were found to be in

close agreement with the measurements. Finally, we demonstrate the 3D knitted helical coil's feasibility for WPT using the coupling between a wound wrist coil and a knitted cuff coil. The attraction of this implementation is that the coil is fully integrated in the garment during its fabrication process. It does not hinder aesthetics, nor does it hinder elasticity or wearability.
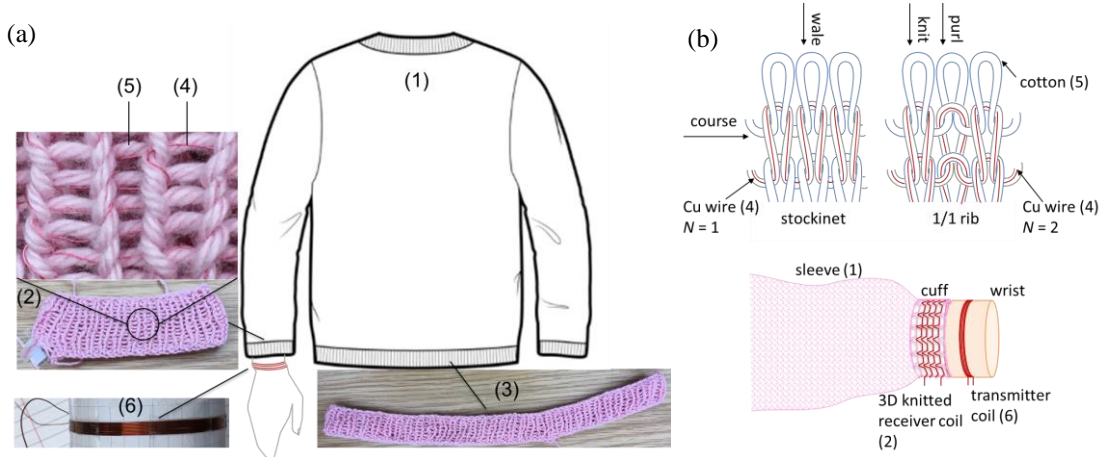

Fig. 1. (a) Illustration of knitted coils in a garment (1). The borders of the garment (2) & (3) are knitted in the round with thin insulated Cu wire (4) and cotton (5) forming the receiver coil(s). Around the wrists or hips, a helical, closely wound coil (6) can act as the primary coil, e.g. in a watch or belt implementation, respectively. (b) top: schematic drawing of the stitches in a stockinet and 1/1 rib knit with identification of the knit parameters. The red line (color online) is the Cu wire. N is the number of rows in which the Cu wire is integrated. Bottom: simplified drawing of WTP between a closely wound coil and a 3D knitted coil in the cuff of a sleeve.

2. Characteristics of knitted coils

In this section, we present the characteristics of single 3D knitted helical coils and derive empirical formulae for self-inductance and resistance. Knitting offers a wide variety of stitches and stich combinations that have a subtle influence on the characteristics of the knitted coil [15, 17]. Standard knits are constructed with knit and purl stitches [18], simple combinations of which give rib or stockinet patterns. In 1/1 rib patterns, purl and knit stitches are alternated within one row. In stockinet, purl and knit stitches are alternated between subsequent rows. Rib is most often used to define the borders of a garment for its simplicity and excellent stretch and stability properties [19].

Analytic expressions for the self-inductance of helical wound coils with a circular cross-section predict a quadratic dependency on number of windings, N and a non-linear dependency on radius r of the form [20, 21]:

$$L = 4\pi N^2 r \times f(r, a) \tag{1}$$

with a the radius of the wire and $f(r,a)$ a logarithmic function of r that is a simplification of the complete elliptic integrals involved.

The resistance of a wound coil is a linear function of the coil radius and the length of the coil, influenced by its pitch. To first approximation (small pitch) R is given by:

$$R \approx 2\pi r N \rho / a^2 \tag{2}$$

with ρ the resistivity of the Cu wire. This equation ignores any radiation, skin and proximity effect [22], acceptable when using thin wires and low frequencies.

The unloaded coil quality factor gives an indication of the losses in the coil:

$$Q = \frac{\omega L}{R} \tag{3}$$

with $\omega = 2\pi f$, the pulsation.

All measurements are carried out using a Wayne Kerr 6500B precision component analyzer with an ac bias of 50 mV and for single coil measurements at a frequency $f = 100$ kHz. The coils are held on cardboard cylinders. The self-resonance of the coils is > 20 MHz and far away from the measurement frequency. Measurements are carried out for the simple wound coils as well as knitted coils in both 1/1 rib and stockinet pattern for $1 \leq N \leq 10$, for different gauge and a diameter, $D = 6.8$. This diameter is approximately a comfortable wrist diameter of an adult male. The yarn used is 4 ply cotton for needles 3 - 3 ¼ mm. All samples are knitted with 3 mm needles by hand in the round except in the study of the influence of the gauge.
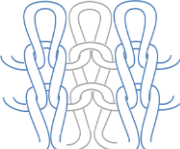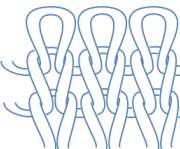
Table 1 gives the influence of the stitch pattern on the self-inductance L, series resistance R and the quality factor Q of the coils. Power fits to the measurements are used to extract self-inductance trends as a function of number of windings. Linear fits are used for the resistance.

The power factor for the wound coil is 1.8, close to the standard analytical equations expected for helical coils, eq. (1). The power factor for the knits is lower at 1.3. This is the result of the larger distance between the courses (rows) in the knit than the closely wound coil, decreasing magnetic coupling. The pre-factor, a function of the radius of the coil and the wire, is higher for the knits. This indicates a different dependence on radius, influenced by the horseshoe character of the knit, especially at the points where the yarn of adjacent stitches overlap. We also observe that the self-inductance of the 1/1 rib is higher than that of

the stockinet, consistent with previous reports [15, 17] and also related to yarn crossings between stitches in a row. The resistance shows the expected linear variation with number of windings, N. Any offset from zero at $N = 0$ is due to the lead-in wires to the coils and incomplete stripping of the insulation of the Cu wire. The resistance of the knit is approximately 4 times larger than the simple wound coil due to the extra wire needed for the horseshoe shapes of the stitches. The length of the yarn needed for rib stitch tends to be slightly higher than that for the stockinet. The quality factor, Q indicates that using the 1/1 rib might be preferable to using stockinet. Thus, in the following study, only 1/1 rib stitch will be used. Further improvement of the quality factor can be obtained by skipping metal wire from some of the stitches to reduce the resistance of the knit. This leads to less wire used but also leads to a reduction in self-inductance and stretchability.

Table 1

Summary of the equations for self-inductance L and resistance R as a function of number of windings, N for $D = 6.8$ cm and different stitch types. Q is derived by ignoring the wire access resistance. The first column shows pictures of the different coils, the second column gives the schematic drawing for the stiches used (the top one is a simple Cu winding).

Picture of coil implementation	Coil type	L (μH)	R (Ω)	Q/ω (1/rad)
	closely wound	$0.3\,N^{1.8}$	$0.3\,N + 0.09$	$N^{0.8}$
	1/1 rib	$0.8\,N^{1.3}$	$1.2\,N + 0.28$	$0.67\,N^{0.3}$
	Stockinet	$0.6\,N^{1.3}$	$N + 0.22$	$0.6\,N^{0.3}$

In knitting, gauge – the number of stitches required per cm length and width – is an important factor influencing drape, stretchability and aesthetics of the resulting garment [23]. Its influence on L and R was investigated by using the same yarn but different sized needles in a coil with $N = 5$ and $D = 6.8$ cm. Only stockinet was used as it enables easy measurements and visualization of the impact of the variation in gauge on the presentation of the garment. The gauge for rib will be different but its impact on coil characteristics follows the same trend with needle size. The results are given in Table 2.

Table 2

Influence of gauge on coil parameters. The knitted coils have $N = 5$ and $D = 6.8$ cm. L_g gives the number of stitches in the length (wale) of the garment and W_g in the width (course). For clarity, the knit picture in the table does not contain the Cu wire.

Picture of knit	Needles (mm)	L (μH)	R (Ω)	L_g (st/cm)	W_g (st/cm)
	4	4.94	5.02	2.9	2.1
	3	4.87	5.06	3.6	2.5
	2	4.75	4.85	5.1	3.1

Increasing the gauge (L_g & W_g), decreases the self-inductance of the knitted coil and decreases its ability to stretch. The closer lying courses with increasing gauge would result in higher L. Since the measurements do not support this intuition, we postulate

that stitch crossover points in the wale direction reduce L due to the opposing direction of the current in these segments. The limited sample length used for the different gauges does not allow a clear picture for the variation of R with gauge but there is indication that a lower gauge requires longer length of wire and increases the resistance.
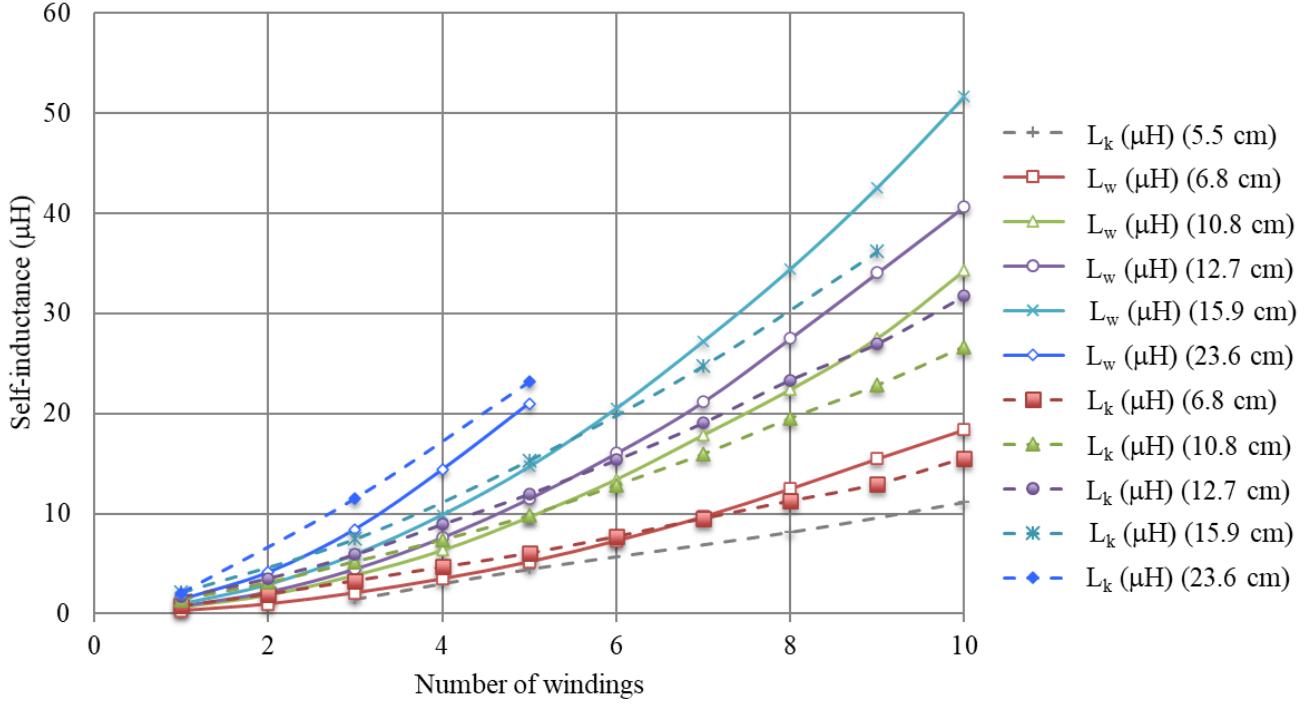

Fig. 2. Measurements of the self-inductance of the coils as a function of number of windings for 6 different coil diameters, D = 5.5, 6.8, 10.8, 12.7, 15.9 and 23.6 cm. L is smallest for the smallest D and its increase with D is monotonic. The dashed lines are the power fits to the measurements (full markers) for the knits and the full lines (empty markers) are for the wound coil. $L_{k,w}$ in the legend is for knitted and wound coil, respectively.

To derive empirical formulae for L and R, 3D helical coils were knitted in 1/1 rib for a wide range of coil diameters D = 5.5, 6.8, 10.8, 12.7, 15.9 and 23.6 cm as a function of windings N. The two smallest diameters are for a female and male wrist cuff, respectively. The larger diameters are for a variety of female and male waist bands. The number of stitches in each coil is adapted according to the gauge for 3 mm needles. Fig. 2 gives L of the wound and knitted coils as a function of N for different D. The dashed lines are the power fits to the knitted coils and the full markers are the measurements. The full lines through the empty markers are the measurements for the closely wound coil. For all diameters, the power factor for the knitted coil is found to be close to 1.3 and for the wound coil close to 1.75, consistent with previous measurements (Table 1). The pre-factor however is dependent on coil diameter as expected from eq. (1). We fit a linear function to the diameter, D. This approach is less complex than that reported in [20, 21], as for $r > 20 \times a$, the factor $f(r, a)$ in eq. (1) can be linearized.

Thus, the analytical equation for L of the wound and knitted coils follows, to good approximation, the following formula:

$$L = (\alpha \times D - \beta) \times N^{\gamma} \tag{4}$$

D is the diameter in cm and N is the number of windings. The parameters α, β, γ are given in Table 3.

The resistance (measurements not shown) varies linearly, as expected. The fits through the measurement, subtracting the leads and contact resistances, give a resistance formula:

$$R = \kappa \times D \times N \tag{5}$$

with constant κ given in Table 3.

Combining eqs. (4) and (5) gives an empirical expression for the quality factor:

$$Q = \frac{\omega(\alpha \times D - \beta) \times N^{(\gamma - 1)}}{\kappa \times D} \tag{6}$$

Table 3
The constants for the empirical formulae of L and R.

Coil type	α (μH/cm)	β (μH)	γ	κ (Ω/cm)
Knit	0.13	0.113	1.3	0.17
Close winding	0.065	0.128	1.75	0.09

These results show that standard closely wound and knitted coils follow a similar behavior for L and R as given by eqs. (1) and (2). The larger separation of the windings and the overlap between yarn for adjacent stitches is causing a difference between the knitted coil characteristics and the standard wound coil, leading to lower power factors and a higher pre-factor. Knitted coils will

always have a higher resistance than wound coils, decreasing their quality factor. This less desirable feature is the consequence of most coil implementations on fabrics that need to remain flexible.

3. Inductive coupling with knitted coils

Measurements of the coupled coils are carried out with two coils on the same cardboard cylinder with a distance measurable in steps of 5 ± 1.5 mm. If the second coil is shorted and the measurement frequency, $f = \omega/2\pi$ is chosen within the range given by [24] (see supplementary data):

$$\frac{R1}{L1} < \omega < \omega_{res} \ \& \ \frac{R2}{L2} < \omega < \omega_{res} \tag{7}$$

then the mutual inductance M can be extracted from:

$$L_{meas} = L1 - \frac{M^2}{L2} \tag{8}$$

$$M = \sqrt{(L1 - L_{meas}) \times L2} \tag{9}$$

with L_{meas} the inductance measured on the first coil and L_1 and L_2 the self-inductance of first and second coil, measured independently.

The coupling factor k can be extracted from:

$$M = k\sqrt{L1 \times L2} \tag{10}$$

and takes a value between 0 and 1 with larger values indicating stronger coupling. For the coils used in this work, the lower boundary for the measurement frequency $f = \omega/2\pi$ in eq. (7) is ~0.3 MHz. The self-resonances of the knitted coils are $f_{res} > 20$ MHz. The measurements are carried out at ~5 MHz, within the range given by eq. (7).

Measurement errors are related to the distance between the coils because the knit never starts with the metal wire in row 1 but is included in row 3 to avoid the knit set-up to influence the inductance (see Fig. 3). Thus, when putting the coils at a distance $d = 0$ cm (adjacent), the knit needs to overlap the wound coil by the 2 first rows, making the distance reading less accurate. In addition, the wire is never positioned in the same manner in all stitches thus if the two coils are adjacent then the distance can still vary between a minimum of twice the wire insulation (~150 μm) and a maximum of the diameter of the yarn (~3 mm). Notwithstanding this variation in zero point, the measurements show smooth variations in function of the different parameters that are studied.
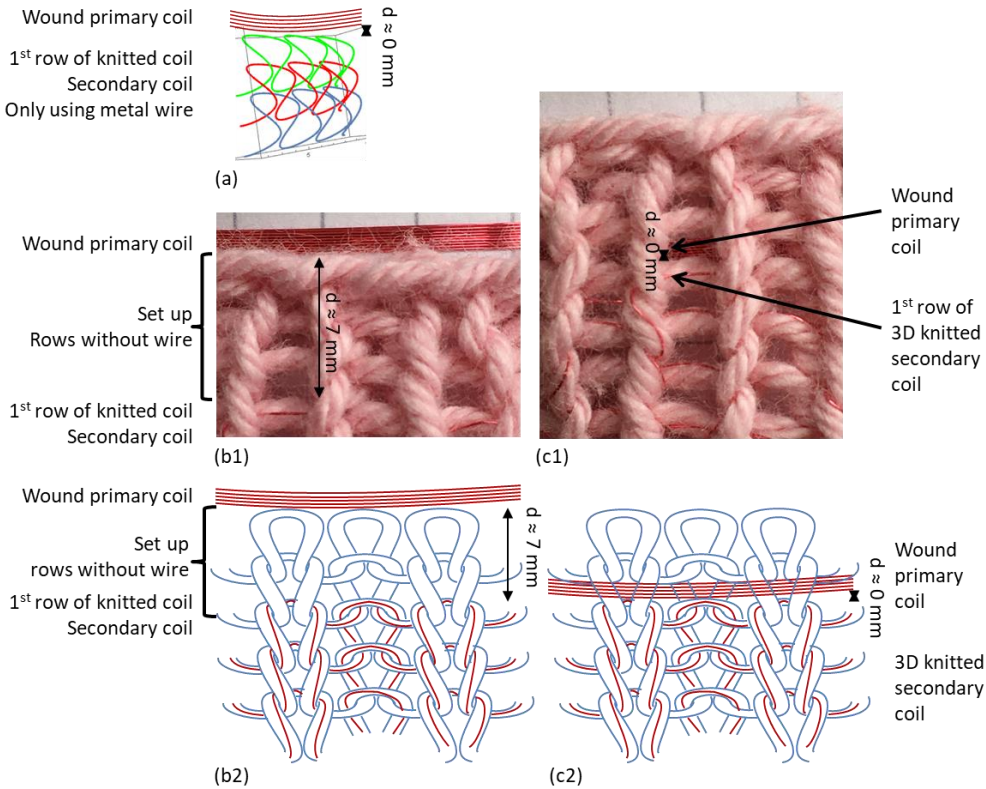

Fig. 3. (a) Gives the knitted coil shape for the simulations and the definition of $d = 0$ mm between wound and knitted coil. Color online: the green is the first knitted row with metal. (b1) The position of the wound coil with respect to the start of the knit. It consists of a set-up row and two rows without wire. These two rows impose a distance of ~6 mm between primary and secondary coil. b2) Schematic drawing of b1). (c1) The $d \approx 0$ mm position for the knit is defined when the knit is shifted upwards over the wound coil to reach a position where the wound coil can be seen through the gap of a stich above the 1st knitted row with metal wire. c2) Schematic drawing of c1). The red lines in b2) and c2) are an illustration of the Cu wire path of the primary wound coil..

The second error is introduced in the approximations of equation (9). The error on the lower boundary is negligible but the error caused by the broad self-resonance (low Q) can be expected to be larger for larger coil diameters that shift f_{res} to lower values.

4. Simulations

To validate the measurements, gain insight in the behavior of the knitted coils and to avoid the need for having to characterize multiple knits in future designs, our Mathematica™ [16] implementation used in [15] was extended to include mutual inductance, M calculations as a function of knit parameters. The simulation of the knit can be tuned by geometrical parameters that are derived from measuring the knitted samples and include: number of stitches per winding, number of windings, the internal diameter of the knitted coil, the thickness of the knit, the distance between the windings and the ratio of the length of the knitted coil to the wound coil. These parameters allow stretch and gauge to influence the calculations. An example of a part of 3 windings of a simulated knit is given in Fig. 3(a) showing three stitches in 3 rows.

In [18, 27] eq. (11) for the self-inductance was used:

$$L \approx \frac{\mu_0}{4\pi} \left(\oiint \frac{d\boldsymbol{x_1} \cdot d\boldsymbol{x_2}}{|\boldsymbol{x_1} - \boldsymbol{x_2}|} \right)_{|\boldsymbol{s_1} - \boldsymbol{s_2}| > a/2} \tag{11}$$

with μ_0 the permeability of vacuum, a the wire diameter, l its length and s measures the length along the wire. This approach showed good first order agreement with the measurements of single knitted coils.

Eq. (11) is derived from the Neumann expression for mutual inductance, given by:

$$M = \frac{\mu_0}{4\pi} \left(\oiint \frac{d\boldsymbol{x_1} \cdot d\boldsymbol{x_2}}{|\boldsymbol{x_1} - \boldsymbol{x_2}|} \right) \tag{12}$$

Eqs. (11) and (12) are very similar with the simplification in (12) that x_1 and x_2 are positions on different coils and no condition is placed on the wire diameter. Therefore, the denominator no longer goes to zero in the calculation of M.

To increase simulation speed of these complex 3D structures the approach taken is to simulate the coupling between a line segment of the wound coil and a stitch of the knitted coil. Summing all these coupled pairs gives M. Results for pairs that are related by rotational symmetry are re-used. To further speed up the simulations, interpolation along the axes of the coils is applied. When comparing the coupling between two wound helixes, M_{hH} - one closely wound (coil 1) and one with windings at a distance of half a stitch height (coil 2) – with that of coil 1 and the knitted coil, M_{hK}, we discover that the difference between the two is mainly due to pairs in close proximity. This means that simulation speed can be further increased by simulating M_{hH} and adding a correction factor that takes the stitch shape for closely spaced pairs into account to obtain M_{hK} with an error smaller than 0.5% for $N > 2$. Thus, for a knitted winding "far" away from coil 1, the influence of the horseshoe character becomes negligible small and the coupling is similar to coupling between 2 helixes with metal wires (as in M_{hH}). This also leads to the realization that the wire shape in the wale direction – parallel to the knit direction – has an impact on the coupling between the coils.

5. Analysis of the mutual inductance

Results of the measured and simulated value M as a function of number of windings, N and coil diameter, D are given in Fig. 4 for adjacent coils.

Fig. 4 confirms that simulations and measurements show the same trend in behavior. Variations in absolute value are mainly due to measurement errors as described in section 3. The errors due to variations in stitch shape in the simulations were shown to be smaller than those due to distance inaccuracies in the measurements.

M increases with N but flattens at higher N. This is because the coupling between coil 1 (closely wound coil) and the windings in the knit further away in distance, is decreasing fast with distance d. M varies approximately linearly with diameter (for larger diameters).
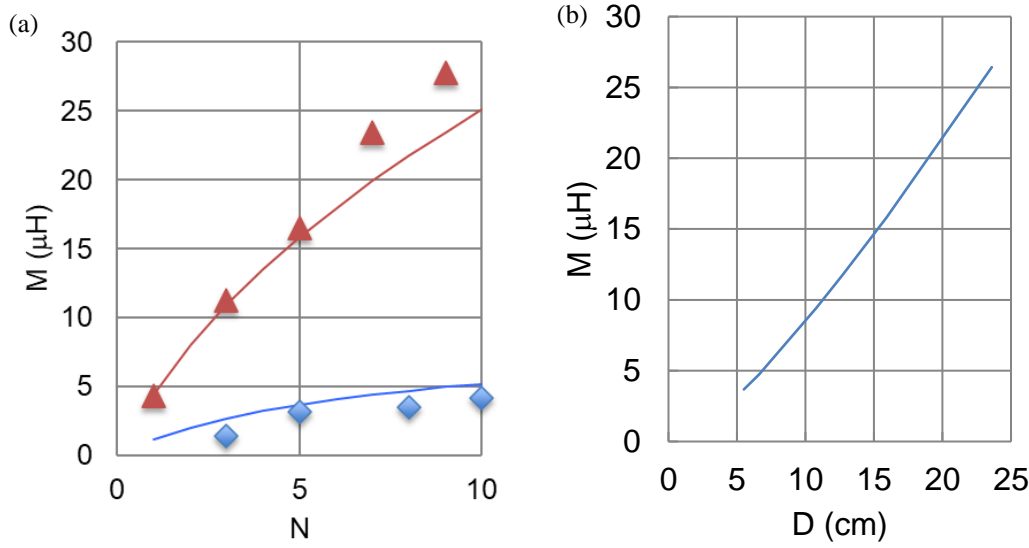
Fig. 4. (a) Measurements and simulation of the mutual inductance M between a standard closely wound coil with $N = 10$ and a knitted coil as a function of number of windings, N for the knit. The coils are adjacent. Measurements are given by markers: diamonds: $D = 5.4$ cm and triangles: $D = 15.9$ cm. Simulations are full lines. (Online color: blue (diamonds) $D = 5.4$ cm and red (triangles): $D = 15.9$ cm). (b) Measurements (markers) and simulations (line) of M as a function of D for adjacent coils for $N = 5$ in the knit.

Fig. 5 gives the measured (a) and simulated (b) values for the coupling factor, k for $D \approx 6.8$ cm and different values of N in the knit. Similar results were obtained for the other diameters (summarized later). The results in the simulations start from 3 mm to take the error in d in the measurement into account (see Fig. 3). The absolute values of k are similar in measurement and simulation and are around $k \approx 0.25$.
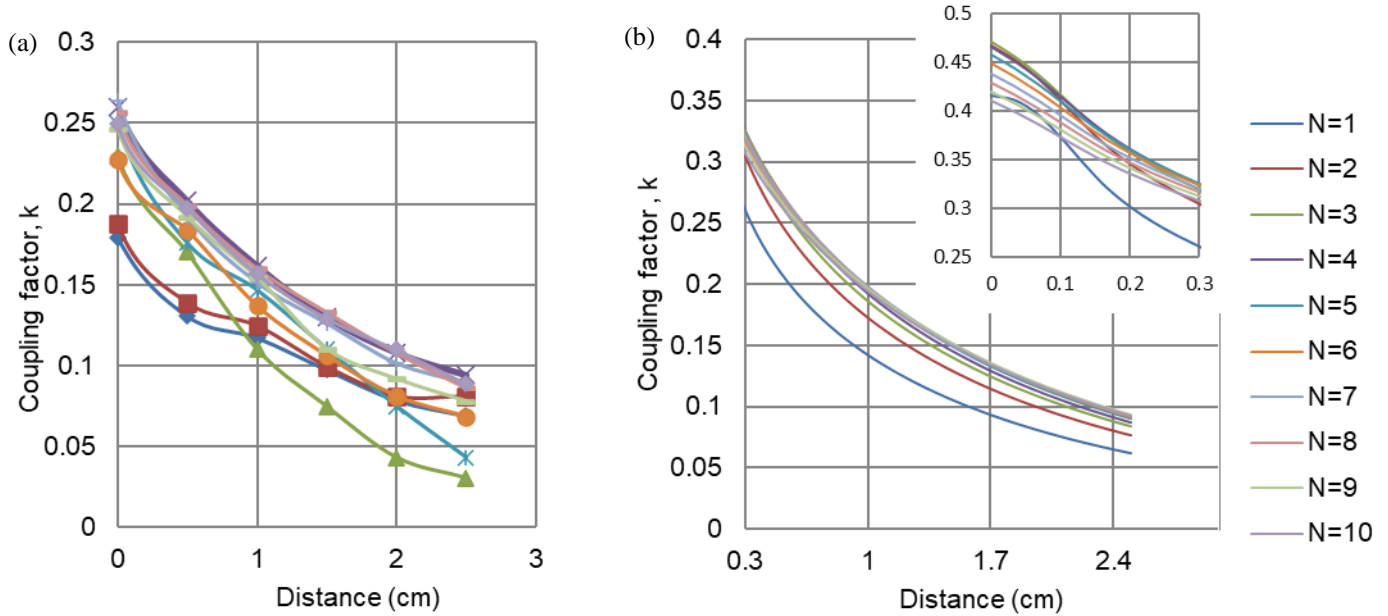

Fig. 5. (a) Coupling factor, k for $D = 6.8$ cm as a function of distance, d for all knitted coils with $1 \leq N \leq 10$. 0 cm is where coils are in close proximity without overlapping (see Fig. 3(c)). b) Simulation of the coupling factor, k for the situation in a). Due to the difference in $d = 0$ mm between measurement and simulation, $d = 3$ mm is chosen to represent a). The inset shows the sensitivity of k at small separation distances. The color coding for N is the same for (a) and (b).

The inset of Fig. 5(b) shows the high sensitivity of k to d for distances smaller than 3 mm. The trend of k predicted by the simulations clearly indicates that for $N = 1$ and 2 the variation with d is different to those with higher N. This confirms the measured trends where k for $N = 1$ and 2 are also lower in value. The reason is the local impact of the knit stitch shape that is not averaged out at low N. An interesting observation is that the coupling factor k for all coil diameters for $N \geq 3$ remains approximately constant. This is because for higher N, the additional windings in the knit lie further away from coil 1 and thus the magnetic coupling decreases and the influence of stitch shape too. This can be used when designing coils for sensors. To maintain a high Q, the number of rows (N) in a knit can be limited to $N = 3$ to 5.

Because the change in behavior of k as a function of d for $N \geq 3$ is small, the average of $<k>$ for $N \geq 3$ is plotted in Fig. 6 for both the measured (a) as well as the simulated (b) values and both for adjacent and overlapping coils. In the case of overlapping coils, the knitted coil overlaps the wound coil approximately symmetrically. In the simulations, the diameter of the knit is increased by 1 mm when it overlaps coil 1. This is a situation easily achieved in reality when the cuff of a garment overlaps a wristband coil. The fits to the measurements and simulations give a logarithmic dependence on D, leading to semi-empirical formulae for the coupling factor as a function of D (for $N \geq 3$):

$k \approx 0.2 \ln(D) - 0.06$ for d ≈ 0 cm (adjacent coils). (15)

$k \approx 0.14 \ln(D) + 0.19$ for overlapping coils.

For large diameters and overlapping coils, strong coupling is observed of the order of $k = 0.6$. Differences in absolute value between measurements and simulations are mainly due to errors of the exact distance between the coils in the measurements.
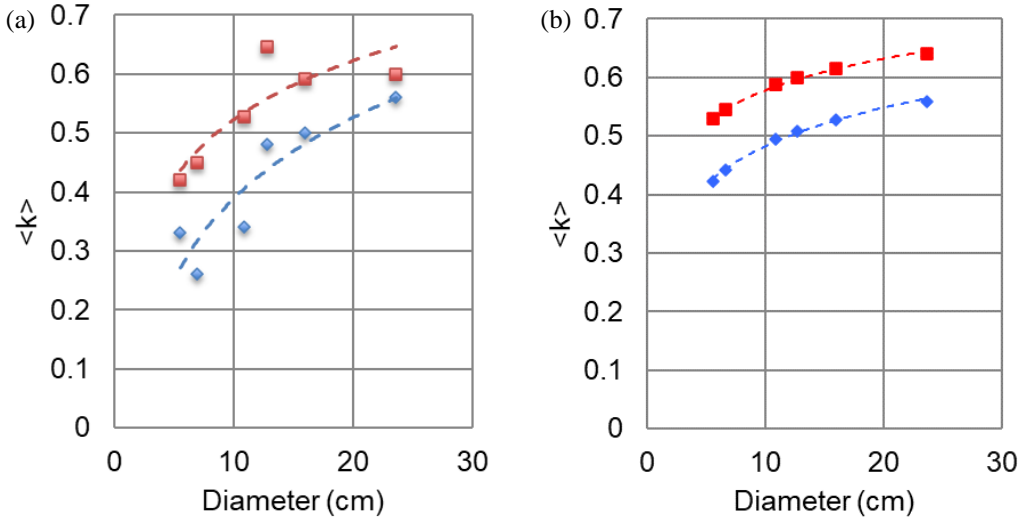

Fig. 6 (a) Coupling factor k as a function of coil diameter. The transmitter coil (1) is closely wound, $N = 10$ and the receiver coil is a knit. $<k>$ is the average of k for $N = 3,4,5,6,7,8,9,10$. Diamonds are for adjacent coils and squares for overlapping coils with the wound coil in the middle of the length of the knitted coil. (b) The results of the simulations for (a). The dashed lines are logarithmic fits to the data points.

To complete the study, M between two knitted coils was also measured and simulated (using stitch pairs). The results are given in Fig. 7.
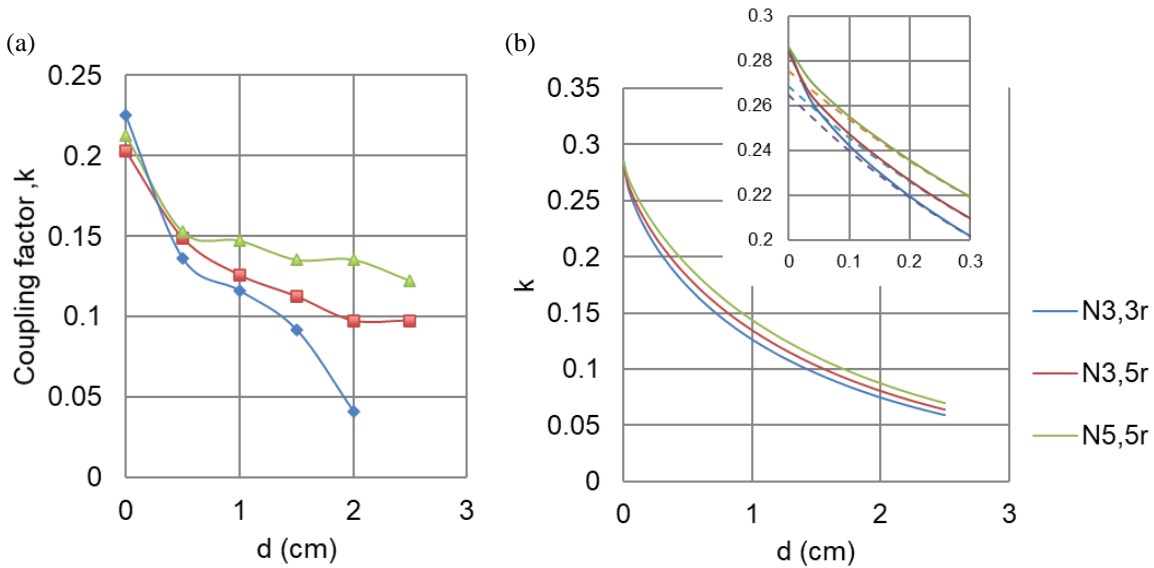

Fig. 7. (a) Coupling factor k between two knitted coils for $D = 6.8$ cm as a function of distance, d. Triangles: both coils $N = 5$, squares: one coil $N = 3$ and the other $N = 5$, diamonds: both knitted coils with $N = 3$. (b) Simulations for (a). The inset focuses on the impact of relative rotation of the stitches at small distances.

We observe that the measured and simulated trends of k vs. d for the knit – knit coupling is similar as that for the wound coil – knit, given in Fig. 5. The value of k for $N \geq 3$ also shows only small differences. In the measurements these variations seem to be larger due to the larger errors in distance determination. Using simulations, we study the effect of aligning the stitches of the two

coils and rotating them over 1 stitch (misaligned). The results are given in the inset of Fig. 7(b). The dashed lines are for aligned stitches and the full lines for misaligned stitches. In the latter case, the currents in the wale direction of the closely spaced stitches in the two coils are in the same direction while when the stitches are aligned they are opposite, resulting in a lower M and thus lower k. The measurements results consist of a variation of relative stitch positions that have an impact on k at small d.

6. Wireless power transfer

One of the possible applications for 3D knitted helical coils is WTP [26]. As illustrated in Fig. 1, the transmitter coil can be a wristband or waistband coil and the receiver coil a 3D knitted coil in the cuff or the waistband of a knitted garment. A 3D knitted coil in 1/1 rib with $N = 5$ with dimensions of a cuff was used to measure power transfer efficiency with a wound primary coil, also $N = 5$, as a function of distance.

Table 4
Measured equivalent circuit elements R, L, C, f_{res} (self-resonant frequency) and Q.

Coil	R (Ω)	L (μH)	C (pF)	f_{res} (MHz)	Q @13.56 MHz
Wound coil	0.5	4.6	7.4	27.3	1458
Knitted coil	5	5.1	4.5	33.2	214

The individual coils were ccharacterized using a HP8753D network analyzer in a frequency range of 0.1 to 80 MHz. The higher frequency range allowed for the measurement of the parasitic parallel capacitor, C. Measurements were carried out with the coils supported by 2 aligned cardboard cylinders that can move to change their relative position (see supplementary data). Table 4 gives the values of the equivalent circuit elements of the single coils (series resistance R, self-inductance L and parallel capacitor, C). The self-resonant frequency, given by: $f_{res} = \frac{1}{2\pi\sqrt{LC}}$ allows for the derivation of C. The quality factor Q is calculated with eq. (3). WPT measurements were carried out at $f = 13.56$ MHz using the circuit given in Fig. 8.
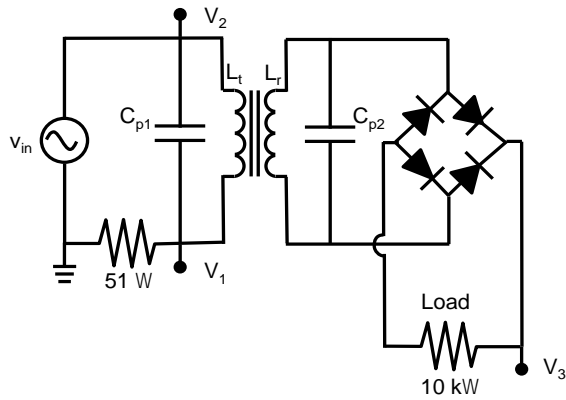

Fig. 8. The equivalent circuit of the WTP system. L_t is the wound transmitter coil. L_r is the knitted receiver coil. C_{P1} and C_{P2} are tuning capacitors. The 51 Ω resistor measures the current in the input circuit. A full wave rectifier is used at the output together with a 10 kΩ load. V_1, V_2 and V_3 are 50 Ω probe connections to the measurement equipment.
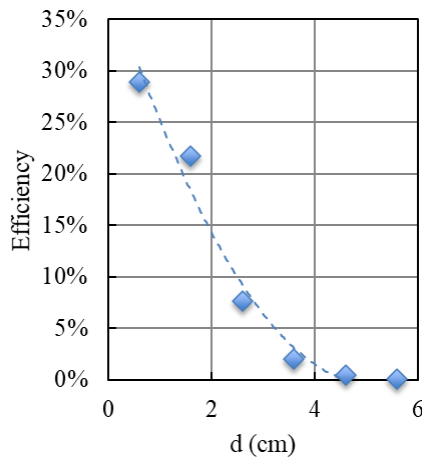

Fig. 9. The WPT power transfer efficiency between the Cu wound coil and the knitted coils as a function of distance. The dashed line is a guide to the eye only.

Breadboards were used to add circuit components for measurements and C_{P1} (33 pF) and C_{P2} (28 pF) for tuning input and output circuit to resonance at 13.56 MHz at a distance d = ~1 cm. A 5 V peak-to-peak AC sinusoidal input voltage at a frequency of 13.56 MHz was supplied using a TTi TG5011 LXI function generator and the DC output voltage and current were measured after the rectifier using an Agilent InfiniiVision DSO-X 3024A digital storage oscilloscope. 50 Ω probes were used for measurements. A 10 kΩ load was chosen, reasonably close to the optimal power point of ~5.5 kΩ at a distance of 1.6 cm between the coils.

Fig. 9 gives the output power efficiency as a function of distance between the primary and the secondary coil. The minimum distance is ~0.6 cm due to the separation of the receiver coil from the transmitting coil by 2 knitted rows without metal. The system efficiency for power transfer is ~30% at ~0.6 cm. This ignores the efficiency loss in the DC-AC transfer that would be required for the transmitter coil to run from batteries. It demonstrates the feasibility of using knitted 3D helical coils in the borders of e.g. a sweater to wirelessly transfer power between a wearable accessory like e.g. a wristband and the garment (see video in supplementary data demonstrating LED light switch on via this implementation).

7. Conclusion

The self-inductance, L and resistance, R of 3D knitted helical coils was investigated in terms of stitch type, gauge, number of windings and diameter of the coil. Empirical formulae were derived for L and R of knitted 1/1 rib and wound coils. These formulae demonstrate the lower power factor for L of the knit due to the larger distance between windings. L's dependence on diameter is nearly linear and stronger than for wound coils, a result of the influence of the shape of the stitches. R of the knit is always larger than for closely wound coils, reducing its quality factor, Q. This feature needs to be taken into account when designing electronics around the coil [27]. Simulations also shed light on the physics aspects of the system, showing that the impact of the shape of the stitches is local. This results in strong dependencies of k to small distance variations for adjacent coils. It also demonstrates an influence of the alignment between stitches of two knitted coils when used for coupling applications. The mutual inductance, M between a wound coil and the knitted coil and between two knitted coils was both measured and simulated. Simulations are able to predict the trend of the variations of M with windings, N and diameter, D. The coupling factors, k showed medium coupling between winding and knit for all diameters between a cuff and waist. When coils are overlapping, the coupling sharply increases in value because an increased number of stitches is in close proximity to the wound coil windings. Due to the larger distance between windings in the knit, k as a function of distance becomes nearly independent of number of knitted windings for $N \geq 3$. This means that for WPT the number of windings can be kept low ($3 < N < 5$) without loss of coupling while maintaining higher Q. A simple WPT experiment was carried out with the coils near resonance at 13.56 MHz, confirming the feasibility of using the knitted coil to wirelessly transfer power between a wristband coil and cuff of a garment. Finally, 3D knitted coils are ultimately wearable as they do not influence aesthetics, elasticity and drape of a garment. Their cylindrical nature conforms both body shapes and helical coil requirements, making them an feasible solution for WTP to supply power to body worn sensor networks.

Acknowledgement

References

[1] T.M. Fernández-Caramés and P. Fraga-Lamas, "Towards The Internet of Smart Clothing: A Review on IoT Wearables and Garments for Creating Intelligent Connected E-Textiles", Electronics 7(12), 405 (36 pp.) (2018).

[2] A. S. M. Sayem, S. H. Teay, H. Shahariar, P. L. Fink and A. Albarbar, "Review on Smart Electro-Clothing Systems (SeCSs)", Sensors 20, 587 (23 pp.) (2020).

[3] S. Lemey,, S. Agneessens, and H. Rogier , "Wearable Smart Objects", IEEE Microwave Magazine, pp. 83-100 Sept-Oct (2018).

[4] Hui, S. Y. R., Zhong, W., and Lee C. K., "A Critical Review of Recent Progress in Mid-Range Wireless Power Transfer", IEEE Trans. Power Electron., **29**, (9), pp. 4500-4511, (2014).

[5] Q.S. Abdullahi , R. Joshi , S. K. Podilchak , S. R. Dhan , M. Chen , J. Rooney , J. Rooney, D. Sun , M.P.Y. Desmulliez , A. Georgiadis and D. Anagnostou , "Design of a wireless power transfer system for assisted living applications", Wireless Power Transfer, 6(1), 41–56 (2019).

[6] Li, Y., Grabham, N., Torah, R., Tudor, J., and Beeby, S., "Textile-based flexible coils for wireless inductive power transmission", Appl. Sci., 8, (6), pp. 912 – 931 (2018).

[7] U-M Jow, and M. Ghovanloo, "Design and Optimization of Printed Spiral Coils for Efficient Transcutaneous Inductive Power Transmission", IEEE Trans. Biomed. Circuits and Syst. **1**(3), pp. 193-202 (2007).

[8] K. Sondhi, N Garraud, D Alabi, D P Arnold, A Garraud, S G R Avuthu, Z H Fan, and T Nishida, "Flexible screen-printed coils for wireless power transfer using low-frequency magnetic fields", J. Micromech. Microeng. 29 084006 (10pp) (2019).

[9] D. Sun, M. Chen, S. Podilchak, A. Georgiadis, Q.S. Abdullahi, R. Joshi, S. Yasin, J. Rooney and J. Rooney, "Investigating flexible textile-based coils for wireless charging wearable electronics", Journal of industrial textiles 0(0) 1-13 (2019)

[10] L. Xu, Z. Liu, X. Chen, R. Sun, Z. Hu, Z. Zheng, T.T. Ye, and Y. Li, "Deformation-Resilient Embroidered Near Field Communication Antenna and Energy Harvesters for Wearable Applications", Adv. Intell. Syst. 1, 1900056 (11 pp) (2019)

[11] Jeong, M. J., Yun, T., Baek, J. J., and Kim, Y. T., "Wireless power transmission using a resonant coil consisting of conductive yarn for wearable devices", Textile Research Journal, 86, (14), pp. 1543–1548 (2016).

[12] M.J. Jeong, K. Park, J.J. Baek, S.W. Kim and Y.T. Kim, "Wireless charging with textiles through harvesting and storing energy from body movement", Textile Research Journal, 89(3) 347–353 (2019).

[13] Sattaluri, D. T., Lo, H., and Ram, R. J., 'Thin thermoelectric generator system for body energy harvesting', *J. Electron. Mater.,* 2012, **41**, (6), pp. 984-988

[14] Y. Zhu, "A wireless power transfer wearable garment," NCSU Libraries Master's thesis, 2016.

[15] Fobelets, K., Thielemans, K., Mathivanan, A., and Papavassiliou, C., "Characterisation of knitted coils for e-textiles', IEEE Sensors Journal 19(18), pp. 7835 - 7840, (2019).

[16] https://www.wolfram.com/mathematica/

[17] Fobelets, K. Knitted Coil for Inductive Plethysmography. Proceedings 2019, 32, 2 (2019).

[18] https://www.merriam-webster.com/dictionary/knit%20stitch

[19] M.S. Choi, and S.P. Ashdown, "Effect of changes in knit structure and density on the mechanical and hand properties of weft-knitted fabrics for outerwear", Textile Res J. 70(12), pp. 1033-1045 (2000)

[20] J.G. Coffin, "Construction and calculation of absolute standards of inductance", Bulletin of the Bureau of Standards 2(1), pp. 87-143 (https://nvlpubs.nist.gov/nistpubs/bulletin/02/nbsbulletinv2n1p87_A2b.pdf)

[21] C. Snow, A Simplified Precision Formula for the Inductance of a Helix with Corrections for the Lead-In Wires, NBS Journal of Research Vol. 9, RP479, June 1932.

[22] J. Ferreira, "Appropriate modelling of conductive losses in the design of magnetic components," in Power Electronics Specialists Conference, 1990. PESC '90 Record., 21st Annual IEEE, 1990, pp. 780–785

[23] A. Charalambus "New approach to a theoretical study of some of the parameters in the knitting process, and their influence on knit-fabric stitch density", AUTEX Research Journal, Vol. 7, No2, pp. 95-99 (2007)

[24] R. Mendes Duarte and G. Klaric Felic, "Analysis of the Coupling Coefficient in Inductive Energy Transfer Systems", Active and Passive Electronic Components Volume 2014, Article ID 951624, 6 pp. (2014)

[25] R. Dengler, "Self inductance of a wire loop as a curve integral", Adv. Electromagnetics 5(1), pp. 1-8, (2016)

[26] K. Fobelets, "Wireless power transfer with knitted coils", E-Textiles 2020, 2nd conference (online) 4 Nov. 2020.

[27] K. Kiener, W. Fobelets, and K. Fobelets, "Respiratory Inductive Plethysmography System using Knitted 3D Helical Coils", E-Textiles 2021, 3rd conference (online) 4 Nov. 2021.